

Supporting Information

Construction of polymer brushes-decorated amphiphilic Janus graphene oxide nanosheets via Pickering emulsion template for catalytic applications

Donghui Cui, Bingfeng Shi, Zhinan Xia, Wenjing Zhu, Changli Lü*

Institute of Chemistry, Northeast Normal University, Changchun 130024, P. R. China.

S1. Materials and Characterization

Material: Graphite powder (99.95%), hydrogen peroxide aqueous solution (30 wt%), saturated sodium chloride solution (6.15 mol/L), trimethylamine aqueous solution (25wt%), tetrahydrofuran (THF, AR, 99.5%), N, N-dimethylformamide (DMF, AR, 99.5%) and 4-nitrophenol (4-NP) were purchased from Aladdin Chemical Reagent Co.Ltd. Pyrene methanol (98%), bromobenzene (AR, 99%), phenylboronic acid (97%), potassium carbonate (K_2CO_3), palladium chloride ($PdCl_2$, 59%-60%), sodium borohydride ($NaBH_4$, 98%), and 4-vinyl benzyl chloride (95%) were obtained from Shanghai Macklin Reagent Co. Ltd. The other chemical reagents were all purchased from Sinopharm Chemical Reagent Co., Ltd. and used as received. (6.15 mol/L)

Chain transfer agent (CTA), S-1-dodecyl-S'-(α,α' -dimethyl- α'' -acetic acid) trithiocarbonate (DDAT) and 5-(2-methacryloyl-ethyloxymethyl)-8-quinolinol (MQ) were synthesized according to the previous literature,^{1,2} N-isopropyl acrylamide (NIPAM, 98%, Macklin) was recrystallized from n-hexane. Styrene (St, 99%, Macklin) was washed three times with 1 % NaOH solution, then washed with deionized water to neutrality, and finally purified by distillation. Azobisisobutyronitrile (AIBN, 98%, Macklin) was used for ethanol recrystallization.

Characterization: Scanning electron microscope (SEM) (Hitachi SU8010) and field emission transmission electron microscope (TEM) (JEM-2100F) were used to observe the morphology of the as-prepared nanomaterials. The sample was prepared by dropping the suspension liquid on the silicon wafer for SEM observation, and the suspension liquid was dropped on the copper mesh for TEM observation. Deuterated

CDCl_3 was used as solvents to obtain ^1H NMR spectra on a 500 MHz AVANCE Bruker NMR spectrometer. X-ray photoelectron spectrometer (XPS, ULVAC-PHI) was utilized to perform the surface chemistry and composition analysis of the sample. X-ray powder diffractometer (Dmax 2200PC) was used to obtain the X-ray diffraction (XRD) pattern. Fourier transforms infrared (FTIR) spectra were measured on Magna 560 FTIR spectrometer and dried KBr tablets were used as blank samples. An inductively coupled plasma atomic emission spectrometer (ICP-AES, LEEMAN Prodigy) was used to determine the content of metallic palladium in Janus nanoparticles. SHIMADZU UV-2550 UV-vis spectrophotometer records the UV-vis absorption spectrum between 200-800 nm. The FV1000 Confocal Fluorescence Microscope (CLSM) was used to observe the morphology of the sample in the oil-water emulsion. The average molecular weights of the as-synthesized polymers were characterized by gel permeation chromatography (GPC) on a Waters instrument (Waters Corporation, USA) at a flow rate of 1.0 mL min^{-1} at $25 \text{ }^\circ\text{C}$ with polystyrene as the standard and THF as the eluent. Digital display high-speed homogenizer (FJ200-S) agitates paraffin-water two-phase at high speed to form the emulsion. Thermogravimetric analysis (TGA) was characterized using a thermal analyzer (Mettler Toledo TGA). Samples were heated from 25 to $800 \text{ }^\circ\text{C}$ in nitrogen with a heating rate of $10 \text{ }^\circ\text{C min}^{-1}$. The Kruss DSA30 droplet shape was used to measure the water contact angle to characterize the wettability of the opposite sides of the Janus nanosheet. Glass slides were cleaned by soaking in $\text{HNO}_3/\text{H}_2\text{O}_2/\text{H}_2\text{O}$ (1:1:1 vol ratio) system for at least 2 h before being rinsed with deionized (DI) water, and then air-

blown dried. To measure the water contact angle of the Janus structure, the Janus nanoplatelet dispersion in DI water was injected into the cyclohexane/brine (4 wt% NaCl and 1 wt% CaCl₂ salt content) biphasic system. An interfacial film was generated through vigorous shaking. A glass slide was used to lift the film from below to capture the film with a hydrophobic surface facing upward. To make the film with a hydrophilic surface facing upward, a glass slide was pressed onto the interfacial film from above and then lifted out. In both cases, the glass slides with interfacial film deposition were dried at room temperature. A drop of water was added to the surface of the sample. After the drop of water stopped spreading, the static contact angle was recorded. Three measurements were taken for each sample.³

S2. Experimental

Synthesis of Pyrene-functionalized RAFT chain transfer agent (Pyrene-CTA) (2).

The DDAT-CTA (1) was synthesized according to methods provided in the literature.⁴ The pyrene functionalized RAFT reagent was synthesized by N, N-dicyclohexylcarbodiimide (DCC) coupling reaction. In short, 0.34 g DDAT-CTA (1), 0.46 g 1-Pyrenemethanol, and 0.06 g 4-dimethyl aminopyridine (DMAP) were added to 20 mL ultra-dry dichloromethane (CH₂Cl₂) solution and mixed. After stirring at room temperature for 20 min, DCC dissolved in 10 mL CH₂Cl₂ was added to the mixed solution, and the reaction ended after stirring for 48 hours. The filtrate was collected by filtration through a funnel. The filtrate was concentrated by rotary evaporation and purified by a chromatographic column using ethyl acetate/hexane (30/70) as the eluent to obtain a yellow oily product, which was dried under vacuum for 24 hours to obtain a yellow solid.

Synthesis of monomer 4-vinyl benzyl trimethyl ammonium chloride (VBTAC).

The monomer VBTAC was prepared by the following steps: 4-chloromethyl styrene (1.68 g, 11 mmol) was dissolved in a mixture of 5 mL ethanol and 3.94 mL trimethylamine aqueous solution (33 wt%). After stirring at room temperature for 2 hours, the solution was dried at 60 °C by an oil pump to obtain the white crude product, which was dissolved in anhydrous ethanol several times. The product was precipitated in hexane and dried at ambient temperature in a vacuum. ¹H NMR spectrum characterization of VBTAC (Fig. S1b): ¹H NMR (500 MHz, D₂O), δ (ppm): 7.66-7.37 (s, 2H), 6.86-6.73 (t, 1H), 5.96-5.83 (d, 1H), 5.42-5.30 (d, 1H), 4.46-4.33 (s,

2H), 3.10-2.97 (s, 9H).

Synthesis of Pyrene-functionalized P(VBTAC-co-St) (3). The prepared 0.113 g VBTAC, 0.385 g St and 0.05 g Pyrene-CTA were added to the three-neck round bottom flask containing 10 mL DMF and mixed. After 30 min of ultrasound, 0.5 mL DMF of AIBN (1 mg mL^{-1}) was added to the reaction system. The reaction mixture was rapidly freeze-thaw cycles three times to remove trace O_2 in the system, and the reactants were stirred in a $70 \text{ }^\circ\text{C}$ oil bath for 24 h. The resulting solution was centrifuged and washed with DMF several times and dried in a vacuum at $80 \text{ }^\circ\text{C}$ to obtain a white sample. The number average molecular weight (M_n) of Pyrene-P(VBTAC-co-St) measured by GPC was 4.8K, and the molecular weight distribution was 1.35.

Synthesis of Pyrene-functionalized PNIPAM (4). NIPAM monomer (1.7 g, 15 mmol), Pyrene-CTA (57.8 mg, 0.1 mmol), and AIBN (8.2 mg, 0.05 mmol) were added to a three-necked round bottom flask containing 3.0 mL of THF. After the system was degassed with N_2 through three freeze-thaw cycles, the system was polymerized at $75 \text{ }^\circ\text{C}$ for 12 h and then purified by precipitation in petroleum ether (120 mL) for three times, and finally, white powder was obtained. The number average molecular weight (M_n) of Py-PNIPAM measured by GPC was 5.4 k, and the molecular weight distribution was 1.24.

Synthesis of Pyrene-functionalized P(NIPAM-co-MQ) (5). NIPAM monomer (1.0 g, 8.85 mmol), MQ monomer (0.08 g, 0.275 mmol), Pyrene-CTA (52 mg, 0.09 mmol) and AIBN (8.9 mg, 0.054 mmol) were added to a three-neck round bottom flask

containing 3.0 mL THF. It was degassed with N₂ through three freeze-thaw cycles, stirred and polymerized at 75 °C for 12 h, and purified by precipitation in petroleum ether (120 mL) for three times. The precipitate was collected by centrifugation to obtain a white powder. The number average molecular weight (M_n) of Pyrene-P (NIPAM-co-MQ) measured by GPC was 4.5 K and the molecular weight distribution was 1.33.

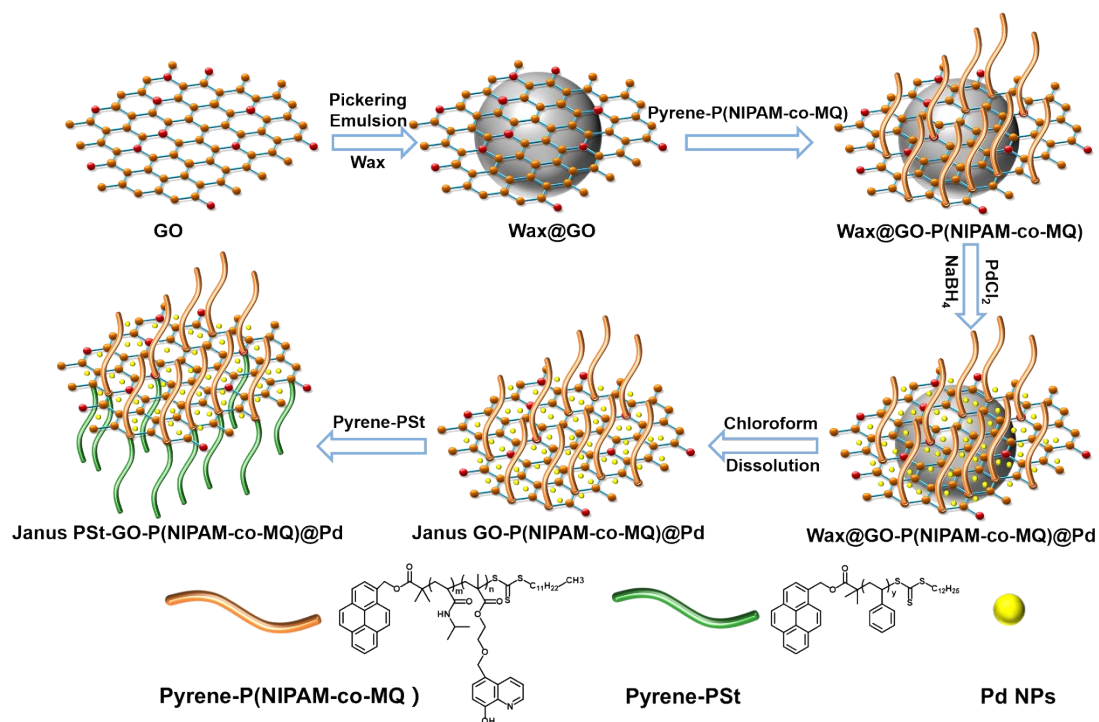
Synthesis of Pyrene-functionalized PSt (6). St monomer (1.04 g, 10.0 mmol), Pyrene-CTA (28.9 mg, 0.05 mmol), and AIBN (6.6 mg, 0.04 mmol) were added to a three-necked round bottom flask containing 4.0 mL of THF. After degassing with N₂ through three freeze-thaw cycles, the powder was polymerized at 70 °C for 12 h, and then purified by precipitation in methanol (120 mL) for three times. The precipitate was collected by centrifugation to obtain a white powder. The number average molecular weight (M_n) of Pyrene-PSt measured by GPC was 5.8 K and the molecular weight distribution was 1.12.

Preparation of GO-P(NIPAM-co-MQ)@Pd nanosheets. GO@Wax (4.8 g) was added to 60 mL of absolute ethanol, ultrasonically dispersed for 2 min, stirred for 30 min, 100 mg of hydrophilic polymer Pyrene-P(NIPAM-co-MQ) was added to the solution and then stirred for 12 h to complete the reaction. The previously configured PdCl₂ ethanol solution (6.0 mL, 0.885 mg mL⁻¹) was added to the solution. After stirring for 2 h, the freshly prepared aqueous NaBH₄ solution (0.2 M, 6.0 mL) was added and continued to stir for 6 h. The obtained product was filtered through a funnel and dried to obtain a crude product Wax@GO-P(NIPAM-co-MQ) @Pd. After the

product was added to the DMF solution for ultrasonic dispersion, chloroform was added to dissolve the paraffin. The liquid was separated through a funnel and centrifuged to obtain the GO-P(NIPAM-co-MQ) @Pd black product, which was washed with DMF and ethanol, and finally dried in a vacuum.

Preparation of Janus PSt-GO-P(NIPAM-co-MQ)@Pd nanosheets. GO-P(NIPAM-co-MQ)@Pd (20 mg) was added to 30 mL DMF solution and dispersed by ultrasonic for 30 min. Then Pyrene-PSt (12 mg) polymer was added to the solution, and the reaction was over after 12 h of stirring. The final sample was obtained by centrifugation, washing, and drying with DMF and ethanol.

Evaluation of the catalytic performance for Suzuki cross-coupling reactions in the aqueous phase. Phenylboronic acid (0.6 mmol), bromobenzene (0.5 mmol), distilled water (5.0 mL), K_2CO_3 (1.5 mmol), and Janus PSt-GO-P(NIPAM-co-MQ)@Pd nanocatalyst (5.1 mg, 0.2 mol% Pd) or Janus PNIPAM-GO-P(VBTAC-co-St)@Pd (4.12 mg, 0.2 mol% Pd) nanocatalyst were added to a 10 mL vial, dispersed ultrasonically and stirred at room temperature for 24 h. After the reaction, the catalyst was collected by centrifugation, and the organic product was extracted with ethyl acetate (10 mL, 3 times). Finally, the reaction yield was obtained by GC.



Scheme S1. Schematic depiction of the preparation of Janus PSt-GO-P(NIPAM-co-MQ)@Pd nanocatalyst via Pickering emulsion template.

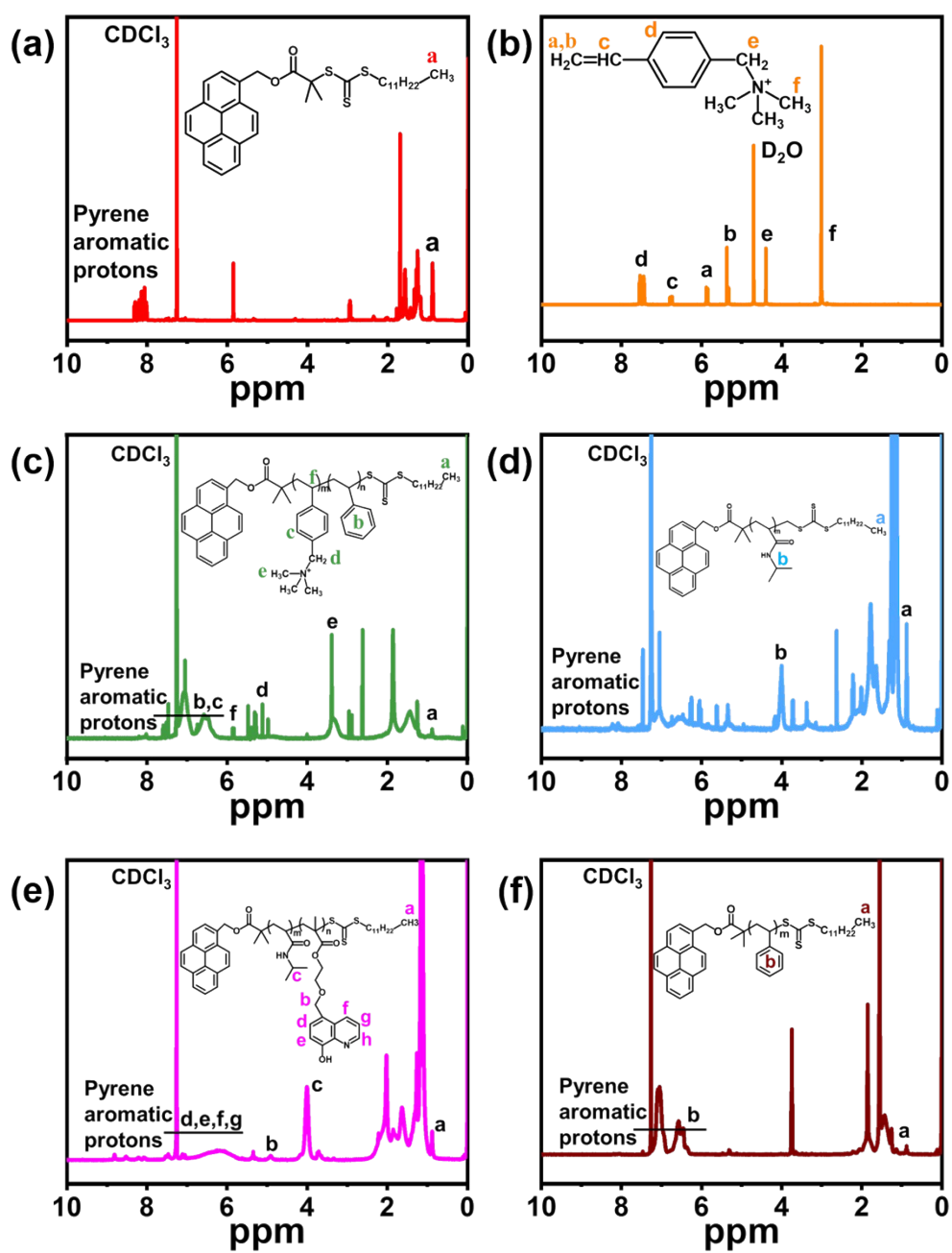


Fig. S1 ^1H NMR spectra of (a) Pyrene-CTA, (b) VBTAC, (c) Pyrene-P(VBTAC-co-St), (d) Pyrene-PNIPAM, (e) Pyrene-P(NIPAM-co-MQ), and (f) Pyrene-PSt.

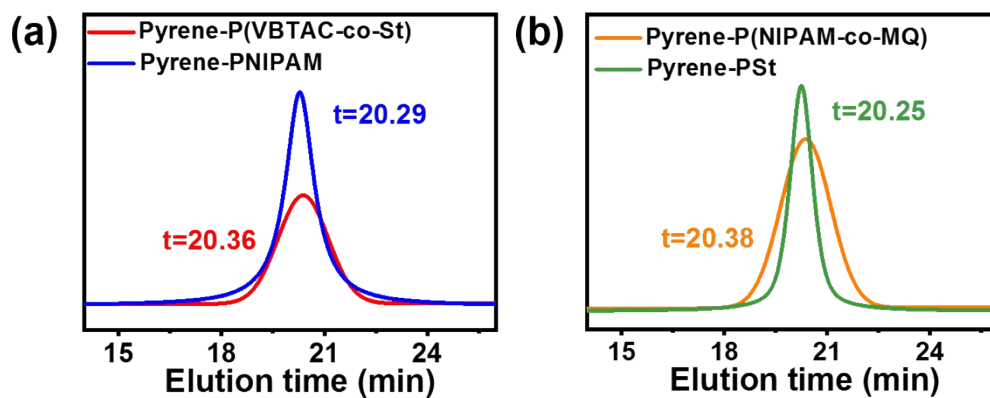


Fig. S2 GPC traces of (a) Pyrene-P(VBTAC-co-St) and Pyrene-PNIPAM polymers, (b) Pyrene-P(NIPAM-co-MQ) and Pyrene-PSt polymers.

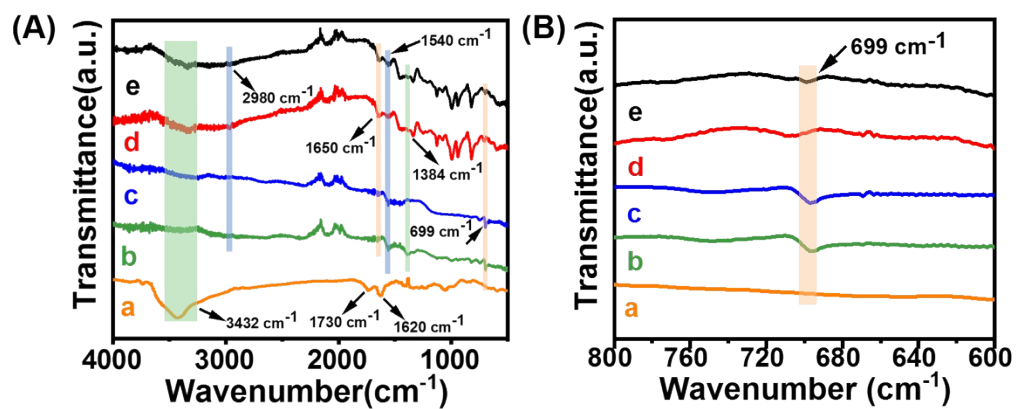


Fig. S3 FTIR spectra (A) and partial magnification (B) of different samples. (a) GO, (b) Janus GO-P(VBTAC-co-St)@Pd, (c) Janus PNIPAM-GO-P(VBTAC-co-St)@Pd, (d) Janus GO-P(NIPAM-co-MQ)@Pd, and (e) Janus PSt-GO-P(NIPAM-co-MQ)@Pd.

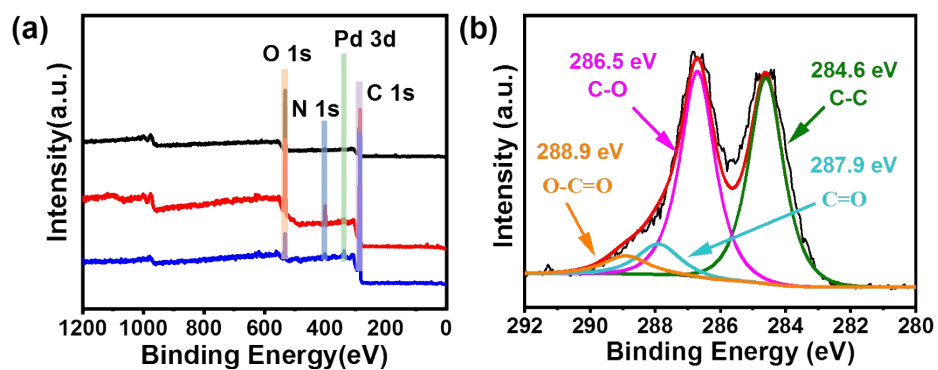


Fig. S4 XPS spectra of a wide scan survey of (a) GO (black), Janus GO-P(VBTAC-co-St)@Pd (red), and Janus PSt-GO-P(NIPAM-co-MQ)@Pd (blue); (b) high-resolution C 1s spectra of GO.

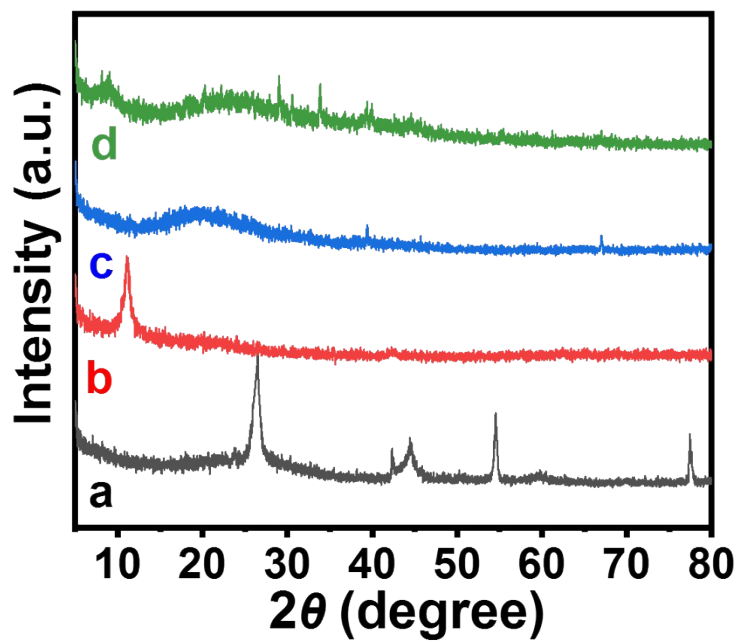


Fig. S5 XRD patterns of graphite (a), GO (b), Janus PSt-GO-P(NIPAM-co-MQ)@Pd(c), and Janus PNIPAM-GO-P(VBTAC-co-St)@Pd (d).

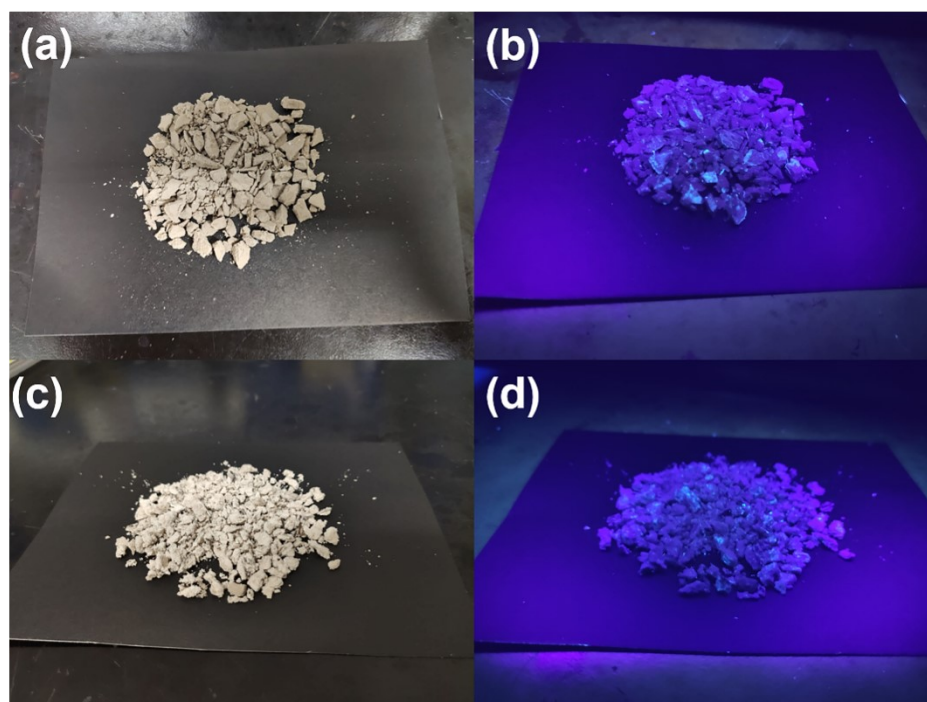


Fig. S6 The photographic images of GO@Wax microspheres grafted with hydrophilic polymer Pyrene-P(NIPAM-co-MQ) (a,b) and hydrophobic polymer Pyrene-P(VBTAC-co-St) (c,d) (The images of b and d were obtained at 365 nm irradiation using a UV lamp).

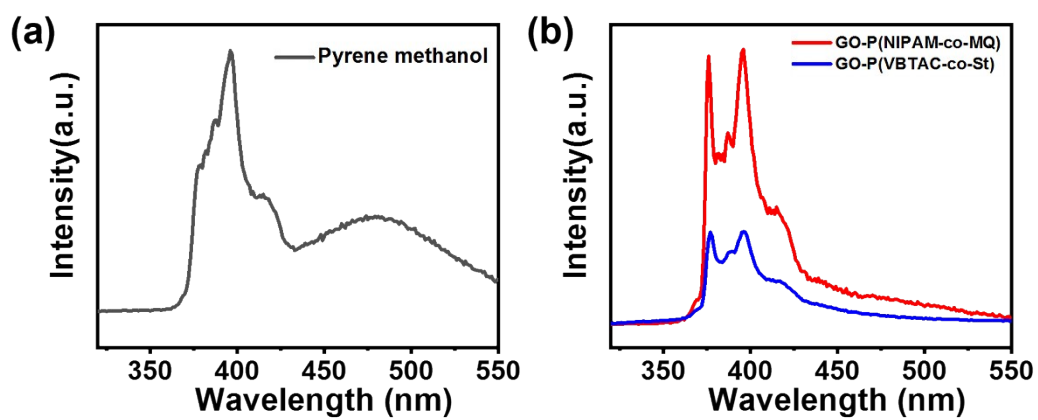


Fig. S7 Solid-state fluorescence spectra at 280 nm light excitation: (a) Pyrene methanol, (b) GO-P(NIPAM-co-MQ) and GO-P(VBTAC-co-St).

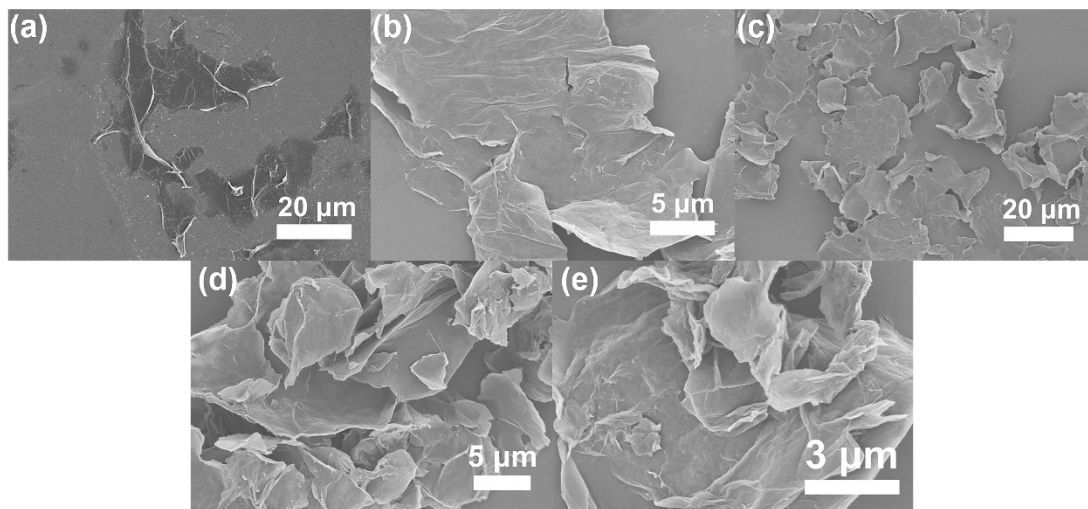


Fig. S8 SEM images of (a) GO, (b) Janus GO-P(NIPAM-co-MQ)@Pd, (c) Janus PSt-GO-P(NIPAM-co-MQ)@Pd, (d) Janus GO-P(VBTAC-co-St)@Pd, and (e) Janus PNIPAM-GO-P(VBTAC-co-St)@Pd.

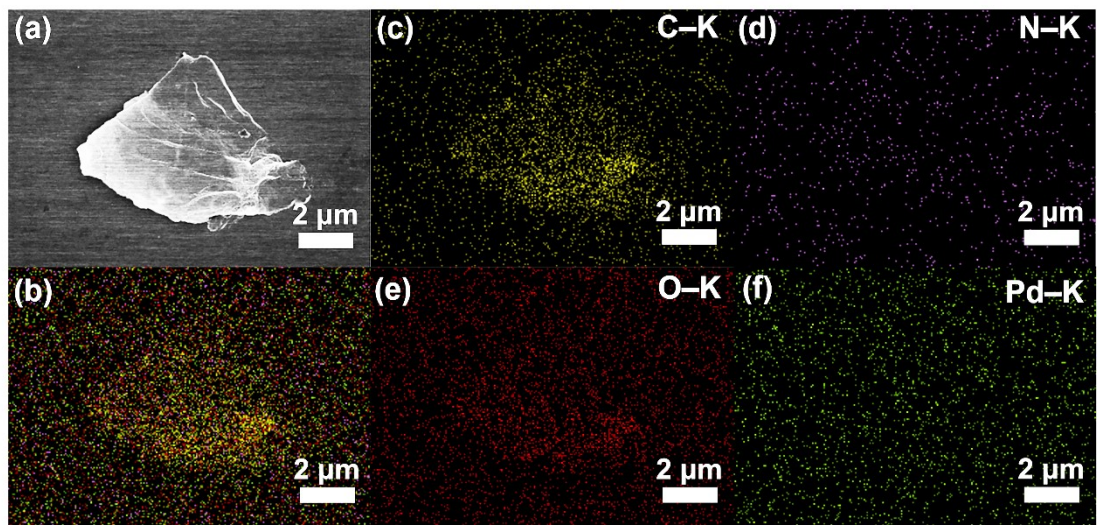


Fig. S9 EDS analysis of Janus PNIPAM-GO-P(VBTAC-co-St)@Pd nanosheets: (a) SEM image, (b) EDS spectrum, and (c-f) EDS elemental mappings of C-K, N-K, O-K, and Pd-K.

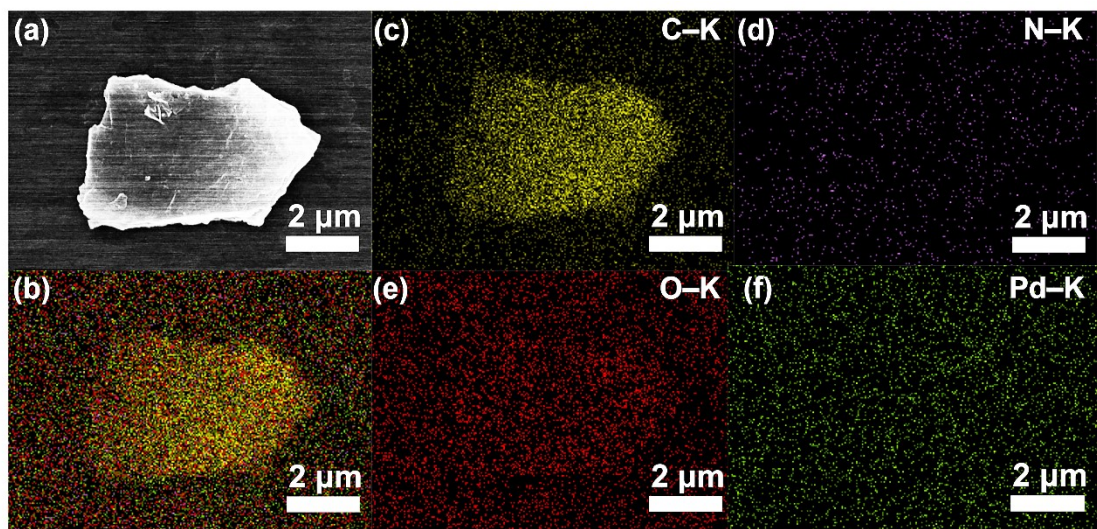


Fig. S10 EDS analysis of Janus PSt-GO-P(NIPAM-co-MQ)@Pd nanosheets: (a) SEM image, (b) EDS spectrum, and (c-f) EDS elemental mappings of C-K, N-K, O-K, and Pd-K.

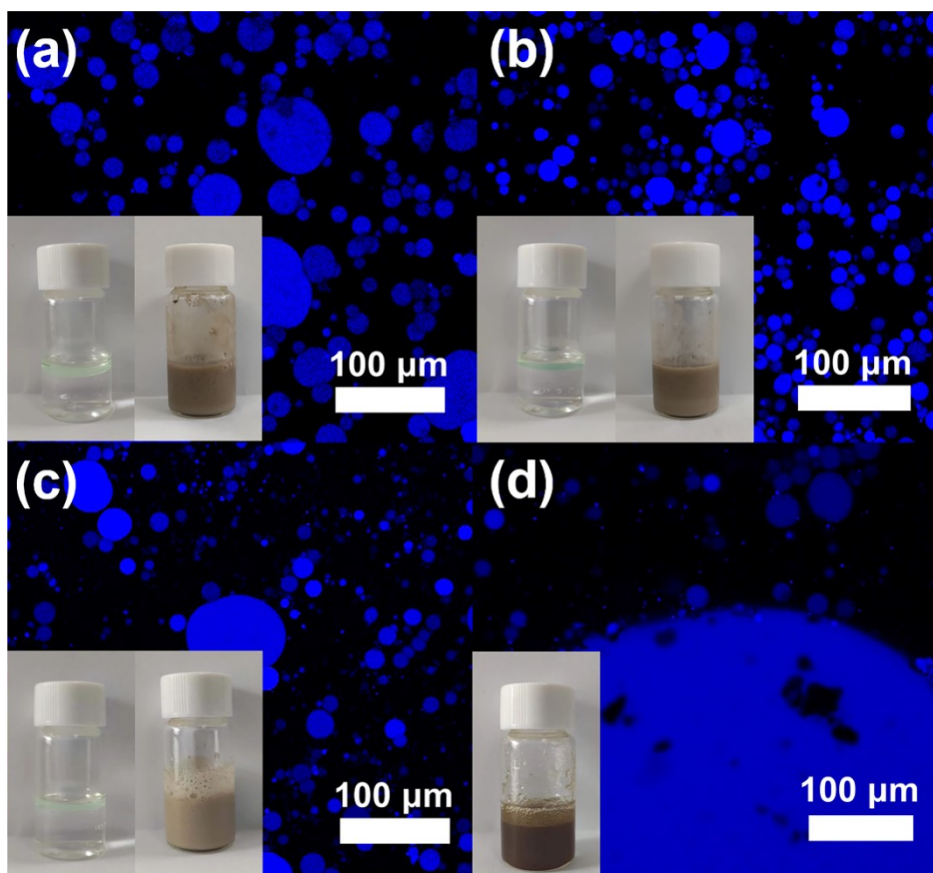


Fig. S11 Test and CLSM images of GO-based nanosheets in toluene/water stable emulsion: (a) Janus GO- P(NIPAM-co-MQ) nanosheet and (b) Janus GO- P(VBTAC-co-St) nanosheet, (c) GO nanosheet, (d) GO nanosheet stabilized emulsions after 30 min (inset: the left vial is a toluene/water two-phase solution, and the right vial is a stable toluene-water emulsion after the addition of Janus nanosheets). For observation, the fluorescent dye coumarin-6 is added to toluene.

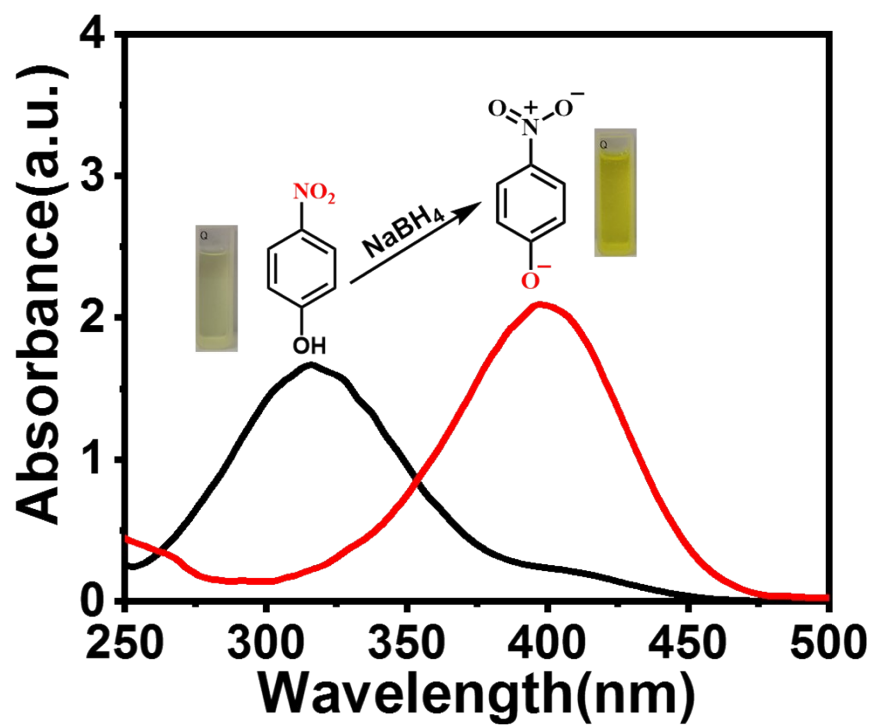


Fig. S12 UV-vis absorption spectra of 4-NP solution before and after adding NaBH₄.

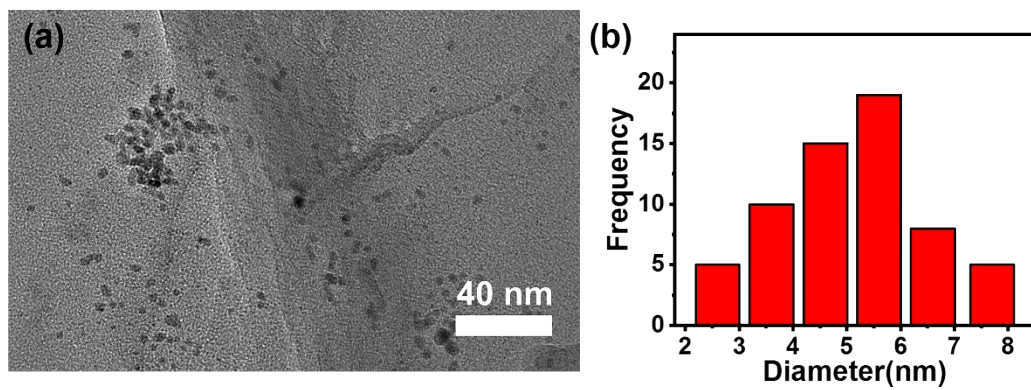


Fig. S13 TEM images (a) of Janus PNIPAM-GO-P(VBTAC-co-St)@Pd (Janus catalyst 2) for 4-NP reduction after five catalytic cycles and surface Pd NPs particle size distribution (b).

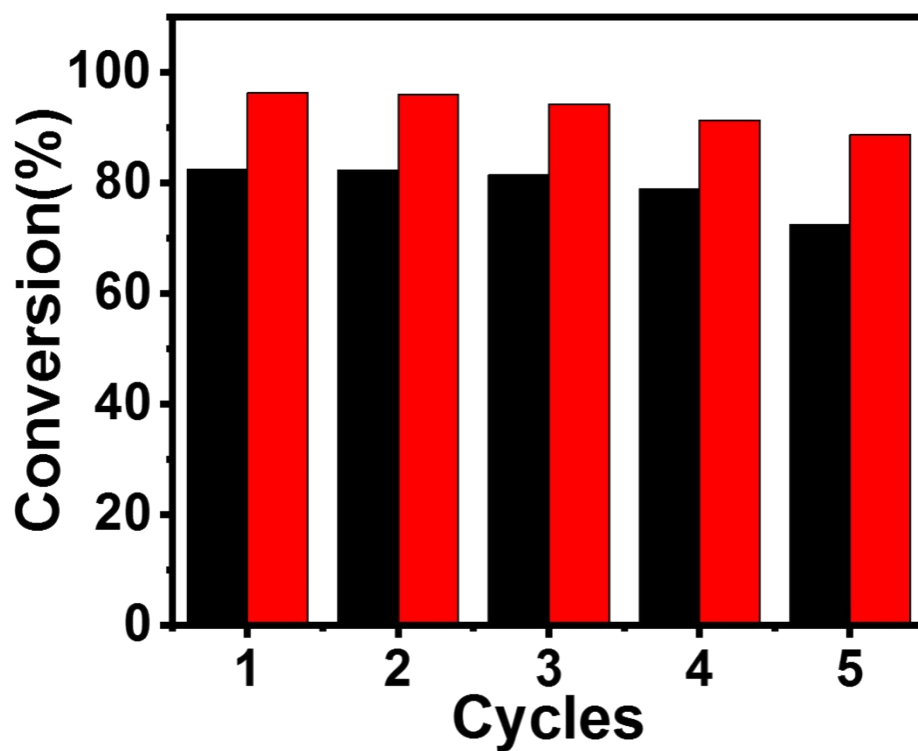


Fig. S14 The reusability of Janus PSt-GO-P(NIPAM-co-MQ)@Pd (black) and Janus PNIPAM-GO-P(VBTAC-co-St)@Pd (red) nanocatalysts for the Suzuki cross-coupling reactions of bromobenzene with phenylboronic acid at room temperature.

Table S1. The calculated molecular weight and dispersity index of the different polymer samples from GPC data.

Polymer	Mn (GPC)	Mn (theory)	Conversion (%)	Dispersity
Pyrene-P (VBTAC-co-St)	4800	6400	42.3	1.35
Pyrene-PNIPAM	5400	6800	70.2	1.24
Pyrene-P(NIPAM-co-MQ)	4500	6200	61.7	1.33
Pyrene-PSt	5800	6500	43.6	1.12

Table S2. Atomic composition of each element in different samples

Sample	C (%)	O (%)	N (%)	S (%)	Pd (%)
GO	68.65	31.35	0	0	0
PNIPAM-GO-P(VBTAC-co-St)@Pd	87.92	8.29	2.62	0.31	0.86
PSt-GO-P(NIPAM-co-MQ)@Pd	81.67	14.35	3.21	0.25	0.52

Table S3. Pd content of Pd from two different Janus nanocatalysts before and after five cycle catalysis based on the data of ICP-AES.

Catalyst	Cycle	Pd content in nanocatalyst (wt%)
Janus PSt-GO-P(NIPAM-co-MQ)@Pd	0	2.10
	5	1.76
Janus PNIPAM-GO-P(VBTAC-co-St)@Pd	0	2.58
	5	2.34

Table S4. Comparison of the ability of various nanocatalysts for the reduction of 4-NP.

Samples	4-NP	Catalyst dosage	Time (min) ^a	<i>k</i> (min ⁻¹) ^b	TOF (min ⁻¹) ^c	Refs
Fe-Fe ₂ O ₃ @PDA@Pd	2.0 mL 2.0 × 10 ⁻⁴ M	30 μL, 0.1 mg mL ⁻¹	7	0.55	75.3	5
MpSi-Pd	1 mL, 1 mM	1 mg mL ⁻¹	20	0.159	1.42	6
Pd/CNs	50 mL, 0.12 mM	0.4 mL, containing 0.04 μmol Pd	10	0.342	14.66	7
Pd/GNS-NH ₂	1 mL 2 × 10 ⁻² M	5 mg, 1.02 wt %	1	-	65.9	8
Mn ₃ O ₄ /PdCu@NC	0.1 mM	0.0015 mmol	-	0.318	12.28	9
NCT@Pd	6 × 10 ⁻⁴ M	1 mg, 0.324 wt %	-	0.67	29.5	10
CNT/PdFe/NC	6 × 10 ⁻² M	3 mg, 1.21 wt %	2.5		70.36	11
Fe ₃ O ₄ @CFR-S- PNIPAM@Pd/CDs	1.0 × 10 ⁻⁴ M	0.02 mg mL ⁻¹ , 40 μL, 3.44 wt %	2.67	1.55	128.6	12
PSt-GO-P(NIPAM- co-MQ)@Pd Janus nanosheets	6.5 μL 1.0 × 10⁻⁴ M	0.5 mg mL⁻¹, 40 μL, 2.1 wt %	4.67	0.81	111.71	This work
PNIPAM-GO- P(VBTAC-co-St)@Pd Janus nanosheets	6.5 μL 1.0 × 10⁻⁴ M	0.5 mg mL⁻¹, 40 mL, 2.58 wt %	4	1.12	142.63	This work

^aThe reduction time of 4-NP in the presence of catalyst. ^bApparent rate constant. ^cTurnover frequency (TOF) is defined as the number of moles of 4-NP reduced per mole of Pd catalyst per min.

References

- 1 C.J. Ferguson, R.J. Hughes, D. Nguyen, B.T.T. Pham, R.G. Gilbert, A.K. Serelis, C.H. Such, B.S. Hawkett, *Macromolecules*, 2005, **38**, 2191-2204.
- 2 N. Du, R. Tian, J. Peng, M. Lu, *J. Polym. Sci. Pol. Chem.*, 2005, **43**, 397-406.
- 3 D. Luo, F. Wang, B.V. Vu, J. Chen, J. Bao, D. Cai, R.C. Willson, Z. Ren, *Carbon*, 2018, **126**, 105-110.
- 4 K. Paek, H. Yang, J. Lee, J. Park, B.J. Kim, *ACS Nano*, 2014, **8**, 2848-2856.
- 5 S. Wang, J. Fu, K. Wang, M. Gao, X. Wang, Z. Wang, J. Chen, Q. Xu, *Appl. Surf. Sci.*, 2018, **459**, 208-216.
- 6 T. Kim, X. Fu, D. Warther, M.J. Sailor, *ACS Nano*, 2017, **11**, 2773-2784.
- 7 X. Wu, C. Lu, W. Zhang, G. Yuan, R. Xiong, X. Zhang, *J. Mater. Chem. A*, 2013, **1**, 8645-8652.
- 8 H.G. Soğukömeroğulları, Y. Karataş, M. Celebi, M. Gülcan, M. Sönmez, M. Zahmakiran, *J. Hazard. Mater.*, 2019, **369**, 96-107.
- 9 Y. Ma, K. Hu, Y. Sun, K. Iqbal, Z. Bai, C. Wang, X. Jia, W. Ye, *Sci. Total Environ.*, 2019, **696**, 134013.
- 10 X.K. Kong, Z.Y. Sun, M. Chen, C.L. Chen, Q.W. Chen, *Energy Environ. Sci.*, 2013, **6**, 3260-3266.
- 11 D. Wang, J. Liu, J. Xi, J. Jiang, Z. Bai, *Appl. Surf. Sci.* 2019, **489**, 477-484.
- 12 Y. Yang, W. Zhu, B. Shi, C. Lü, *J. Mater. Chem. A*, 2020, **8**, 4017-4029.